Aquavoltaic system for harvesting salt and electricity at the salt farm floor: Concept and field test

Article *in* Solar Energy Materials and Solar Cells · October 2019

DOI: 10.1016/j.solmat.2019.110234

1 author:

Jongsung Park
Gyeongsang National University

Solar Energy Materials & Solar Cells 204 (2020) 110234

Contents lists available at ScienceDirect

Solar Energy Materials and Solar Cells

journal homepage: http://www.elsevier.com/locate/solmat

Aquavoltaic system for harvesting salt and electricity at the salt farm floor: Concept and field test

Bongsuck Kim [a], Seung-min Lee [a], Seong-hyun Kang [a], Moon-sun Jeong [a], Geun Ho Gim [b], Jongsung Park [b,**], Cheolhyun Lim [b,*]

[a] Korea Electric Power Research Institute, Naju-Si, Jeollanam-do, 58217, Republic of Korea
[b] Green Energy Institute, Mokpo-Si, Jeollanam-do, 58656, Republic of Korea

A R T I C L E I N F O

Keywords:
Aquaovoltaic
Salt farm
Photovoltaic
Module
Electricity
Energy harvesting

A B S T R A C T

The concept and design of a photovoltaic system for harvesting salt and electricity at salt farm floor were proposed for the first time. Various concepts and designs were explored from the point of view of waterproofing, salt resistance, material and electrical safety, maintenance, and economic feasibility. Even though the concept and design are still evolving through field tests, the first-generation design of a photovoltaic system applied on the salt farm floor is unveiled. The power generation of the salt-farm parallel system is comparable to that of conventional solar power plants. The cooling effect by seawater contributes more to the increase in the crystalline silicon photovoltaic module performance than does the absorption loss due to seawater by maintaining a certain height above the module.

1. Introduction

In this age of climate change crisis, energy conversion from fossil fuels to renewable energy is a natural choice for mankind [1,2]. Although renewable energy is a cost-constrained supply of new and renewable energy, some countries have successfully increased their rates of renewable energy by utilizing their own renewable energy resources and government-support policies based on social consensus and economic power [3–5]. The energy import dependency of South Korea stood at 94.7% in 2016, corresponding to 809.4 billion dollars [6] in energy imports. Therefore, the energy trend shift of South Korea from fossil fuel to renewable energy is unavoidable. However, it is true that there is still a lack of national consensus on energy transition from fossil fuel to renewable energy. This is because solar power plants are generally installed in farming and fishing villages, causing environmental damage [7,8], and the nation's land area is limited for the installation of solar power plants [9]. However, the three borders of South Korea are surrounded by the sea, therefore, there is high potential for installation of solar power plants at seashores. Furthermore, the salt-farming industry is well-developed because of the large available salt ponds at the seashore; the total area of salt fields in South Korea is about 46 million square meters. Despite the superiority of the salt industry in South Korea, the selling price of salt is less than half of the production cost because of the collapse of the industry itself. A yeomjeon (a salt farm in the Korean language) is an ideal location for solar power generation because of its large amount of sunlight and strong winds; many businesses thus desire to utilize it for solar power plants. Salt farmers offer their sites to businesses, being unwilling to produce salt because financial losses. Therefore, stable additional profits for salt farmers is necessary in order to retain the nation's leading salt farm industry are available. If underwater solar power modules are installed at these sites, then it is expected that solar power plants could produce 4 GW of electricity.

For these reasons, we propose in this research the concept of a salt-field parallel solar power system, which can combine salt production and solar power generation at the same site, the first of its kind. Salt fields mainly consist of three stages: reservoirs, evaporating ponds, and crystallizing ponds. The salinity of seawater entering the reservoir is 1%–3%; it is then moved to the evaporating ponds, where suspended solids sink in the reservoirs. Evaporating ponds take up ~85% of the entire salt field, and they have two different zones. In the first zone, the salinity of the seawater gradually increases from 3% to 8%; in the second

* Corresponding author.
** Corresponding author.
E-mail addresses: kbs74@kepco.co.kr (B. Kim), sm.lee@kepco.co.kr (S.-m. Lee), shyun.kang@kepco.co.kr (S.-h. Kang), moonseon@kepco.co.kr (M.-s. Jeong), ggh1242@gei.re.kr (G.H. Gim), jspark@gei.re.kr (J. Park), chlim@gei.re.kr (C. Lim).

https://doi.org/10.1016/j.solmat.2019.110234
Received 11 May 2019; Received in revised form 13 August 2019; Accepted 13 October 2019

zone, it increases from 8% up to 18%. The concentrated seawater is stored in a water storage container (Haeju, Korea), and it is distributed to its destination, salt crystallizing ponds, where the salinity reaches about 27%–30%. A salt farm adopting a solar evaporation method in South Korea conventionally consists of two ponds: an evaporation pond for increasing salinity and a crystallization pond for harvesting salt, as shown in Fig. 1 (a). The proposed salt-field parallel solar power system is shown in Fig. 1 (b). It is a concept in which the large waterproof tank of a solar module is installed at the bottom of an evaporator that contains only 3°–18° of saline concentration saltwater at a height of 10–20 cm. It simultaneously increases the salinity of the saline water.

We assume that there are two main advantages of using solar modules under seawater in salt farming. First, it helps evaporate water, as solar modules generate heat in the process of producing electricity, resulting in increased production of salt [10]. Second, seawater has a cooling effect on the crystalline silicon module, as the temperature of the seawater is much lower than that of solar modules, thus improving the overall performance of the solar modules [11–13]. The photovoltaic (PV) system installed in this project on the salt farm floor could be launched because of the support of the salt industry, which has suffered from the salt price slump in South Korea. Throughout experiments, we found that the electricity generation rate of the salt-farm modules was higher than that of the land-installed modules (0°, reference module). The seawater contributes more to the increase in the module performance than did the absorption loss due to water by maintaining a height of 2 cm above the module. The salt-farm parallel system showed an annual power generation higher than that of the land-installed modules (0°, reference module) and similar to that of the land-installed modules (30°).

2. Experimental

2.1. The design concept of the salt-farm parallel solar power system

In order for PV modules to play a role as an evaporating pond, it is necessary for the entire surface of the solar modules to contain salt water and to be capable of releasing the salt-containing water for the next process when the saline concentration is increased. To do this, we fabricated a large waterproof vessel composed of a photovoltaic module that can contain salt water. We used tempered glass for the front side of the modules, which is in contact with the salt water. The water vessel was made of salt-resistant material with high thermal-shock strength and fiber-reinforced plastic (FRP), and the sidewall of vessel had a 30° angle in order to prevent shading of the solar modules. The gaps between solar modules were filled with waterproofed rubber filler and edible silicone. Seawater could be loaded up to 20 cm height in front of the module in the vessel, and it had an automation system that automatically transports seawater from the vessel to the next step. Since the solar module was installed horizontally to the ground, it was designed to make it float at a certain height from the bottom and to adjust the height in consideration of the effect of low geothermal heat, humidity generated in the earth, and ease of maintenance. If perfectly waterproofed PV modules are submerged even in the shallow water (less than ~30 cm depth), it would be realistically hard to operate them for more than 20 years in the seawater. In addition, maintenance and cleaning of modules contaminated with mud from the salt farm floor is not easy. Therefore, our concept is that the huge vessel is able to hold seawater of ~20 cm in height, with the top constructed from waterproofed PV modules. This PV module vessel functions as an evaporation pond. The modules are installed at a height of ~40 cm from the salt farm floor for long-term reliability and low maintenance. The gaps between modules are sealed with specially designed parts to prevent the leakage of seawater. The design concept is shown in Fig. 2.

2.2. Characterizations

In order to examine the feasibility of the underwater solar photovoltaic module, we prepared an indoor test system. Three types of single-crystal silicon cells were modularized through lamination, and a polycarbonate water tank was fabricated and installed on the floor where they were inserted. For water temperature and depth control, the water temperature was controlled using the constant temperature water tank, and this was monitored through a thermometer attached to the surface of the module. A flow meter was used to control the rate of flow into the constant-temperature water tank. The temperature of the water was 10–40 °C, and the height of the water was 0 cm–10 cm. A solar simulator (k201 LAB50, South Korea) was used to measure the *I–V* characteristics of the modules installed in the water tank at 1000 mW/m^2 irradiance.

3. Results and discussion

3.1. Indoor tests

First, we measured solar irradiance loss at different depths from the sea level in order to estimate the optical loss of the solar modules installed at different depths from sea level. Fig. 3 shows the spectral solar irradiance measured at different depths from sea level. The spectral solar irradiance was measured at the surface of the sea level (0 cm, reference) and at 2, 5, 10, and 20 cm. As can be seen in the figure, solar irradiation at 300–600 nm was not changed along with depth. Unlike in the 300–600 nm wavelength range, the spectral solar irradiance decreased with increased depth. It is obvious that the sea water had light absorption [14], so that solar irradiation decreased as the sea water depth increased. In order to estimate the current density of the solar cell located at different depths from the sea level, we measured the spectral solar irradiance (Fig. 3 (b)). As shown in Fig. 3 (a), the solar irradiance decreased as the depth from the sea level increased. This is mainly due to the parasitic absorption of the seawater. In order to calculate the current density of the solar cell located at different depths, we used spectral mismatch calculation available at the PV lighthouse (www2.pvlighthou

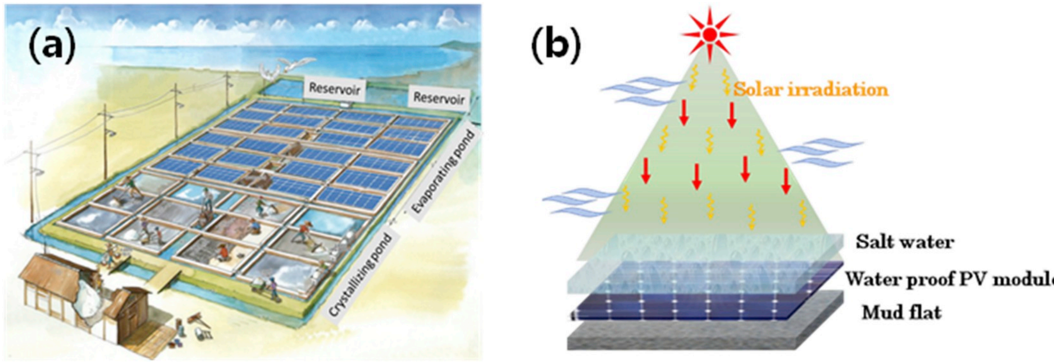

Fig. 1. (a) Schematic diagram of general salt farm in South Korea, and (b) Schematic diagram of proposed salt farm parallel solar power system.

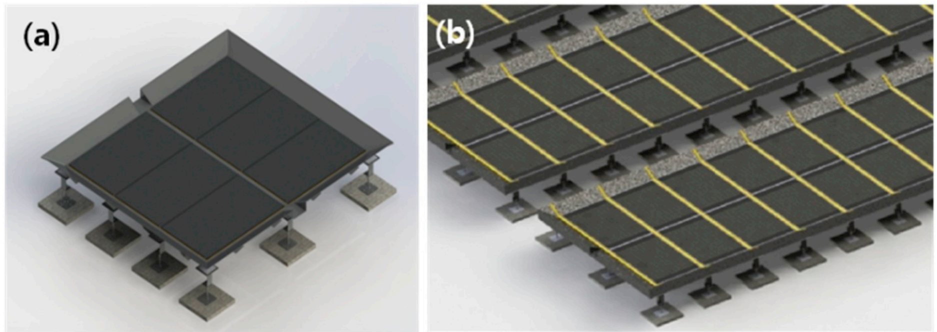

Fig. 2. The concept of the sea water vessel act as an evaporated pond in salt farm (a) single vessel, and (b) interconnected vessels.

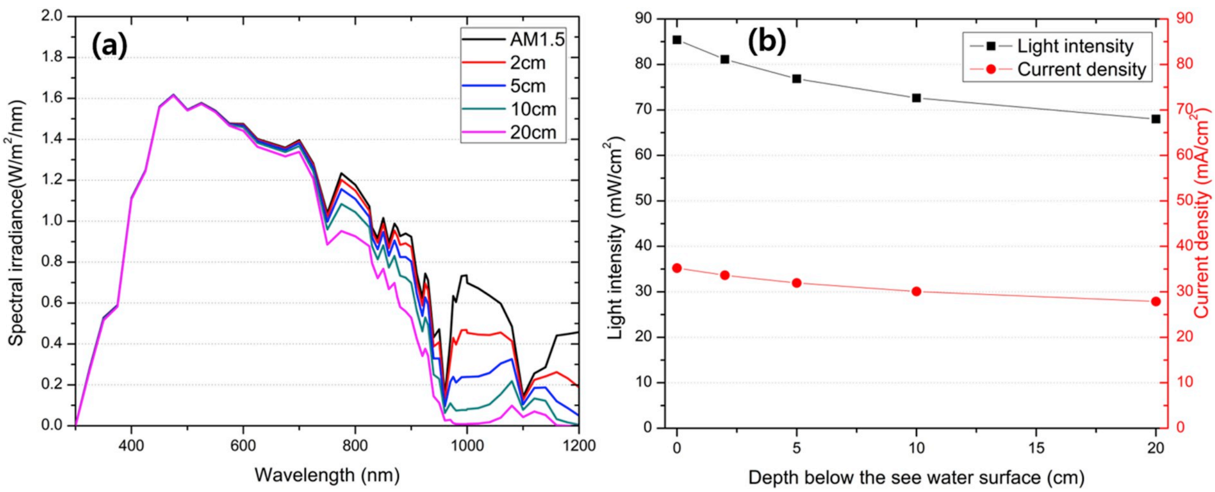

Fig. 3. (a) Spectral solar irradiance at different depth from the sea level, and (b) light intensity and calculated current density of c-Si solar cell in different depth below the sea surface.

se.com.au). We used standard screen-printed solar cell for this calculation. The current generation at long wavelengths varies depending on the cell architecture (i.e., screen-printed solar cells, PERC, and IBC cell). Therefore, the quantum efficiency at long wavelengths differs from the different cell architectures. However, if a single type of solar cell is selected for the calculation, it is possible to estimate the changes in current density with varying solar irradiance. It can be seen in Fig. 4 that the current density decreases as the light intensity decreases. In addition, the reduction width of the light intensity and reduction width of the current density with the depth of water showed nearly the same tendencies. The current density at AM1.5 was 35.22 mA/cm^2, and it decreased to 33.65 mA/cm^2 at 2 cm below the water (4.46% reduction) and decreased to 27.87 at 20 cm below the water (20.88% reduction). We can deduce, therefore, that the reduction in current density is due to the reduced light intensity above 700 nm. The details of the current density calculation results are shown in Table 1.

Fig. 4 shows *I–V* curves of the c-Si mini module at different depths from the sea surface. For this measurement, the samples were positioned at 2.5 cm intervals from 0 cm, which is the control, up to 10 cm. It can be seen in the figure that only the current density (here, current) decreases as the depth increases. The current densities (cell area: 243.4 cm^2) of the samples at 0, 5, and 10 cm are 36.27, 30.28, and 27.12 mA/cm^2, respectively. The current density from the *I–V* measurement is close to that of the calculated current density shown in Table 1. As depicted in Fig. 3, the light irradiance decreased as the depth increased, such that we observed a current reduction from the *I–V* measurements. Due to current density losses, open circuit voltage (V_{oc}) is also slightly decrease. This is because light intensity decreased in this measurement. Therefore, the measurement results agree well with our expectation. Here, the depth of the samples from the sea surface was linearly increased in the same interval, 2.5 cm, but the current was not linearly reduced. This is because light absorption of the seawater is not linear as depth increases, as shown in Table 1.

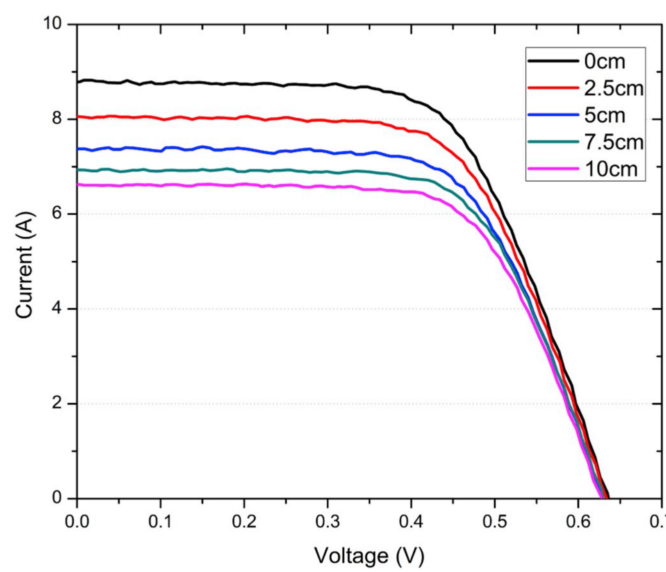

Fig. 4. *I–V* curves of c-Si mini modules located at different depth below the sea level.

Table 1
Calculated current density of c-Si solar cell in different depth from the sea level.

	AM1.5	2 cm below sea level	5 cm below sea level	10 cm below sea level	20 cm below sea level
Measured light intensity (mW/cm^2)	85.44	81.12	76.86	72.63	68
Calculated current density (mA/cm^2)	35.22	33.65	31.95	30.09	27.87
Decrement of current density (%)	0	−4.46	−9.28	−14.56	−20.88%

Fig. 5 shows the correlation between water depth, water temperature, and efficiency of the Si minimodule. It is well known that temperature affects the overall performance of solar cells. For c-Si solar cells, the current increases slightly with temperature, while voltage and fill factor decrease with temperature, which more significantly affects the performance of the cell. As discussed above, current decreases as the water depth increases, and so the overall efficiency decreases with water depth. In the case of temperature variation, efficiency increases with the water temperature decrease, which is in good agreement with previous reports. Interestingly, the reduction width by temperature is nearly close to that of the samples at different water depths. Therefore, it can be said that there is no strong correlation between water depth and temperature in terms of the module efficiency. We assume that water depth and water temperature independently affect the module performance.

Fig. 6 shows the dependency of the solar cell efficiency on the type of water and on the salinity of the seawater. The salinity of the seawater increases as it moves to the next stage, and so it may have effects on the performance of the solar modules. In order to test this, solar modules were immersed in different water samples: tap water and seawater (salinity of ~10%). As can be seen in Fig. 6 (a), the normalized efficiencies of the solar modules in the different water samples were close to each other at the same depth. The module in salt water shows slightly lower efficiency (<1%), which is negligible. This agrees well with a previous report [15]. We also tested the efficiency dependence on the salinity of the seawater. It can be seen in Fig. 6 (b) that there is a slight decrease in normalized efficiency with increased salinity, which agrees well with the results in Fig. 6 (a). Therefore, we can conclude that the salinity does not have a strong effect on the performance of solar modules in the short term. In addition, the long-term effects of salinity on the performance of solar modules should be further investigated.

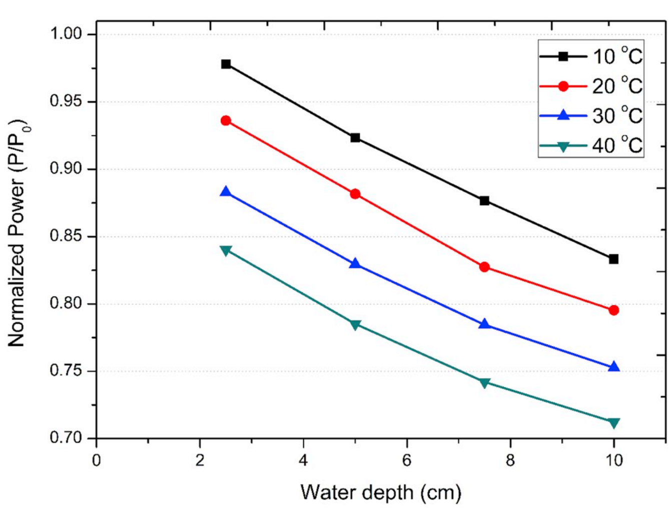

Fig. 5. Correlation between water temperature/water depth and normalized efficiency of the Si module.

3.2. Field tests

Fig. 7 shows an image of the salt farm parallel solar power system installed at our test site. As can be seen, the system is installed in an environment similar to actual salt ponds; this makes it easy to supply the seawater and exposes the solar power system to the harsh sea environment. In this test bed, we designed a pilot system that can accommodate various types of solar cells and modules for further intensive study. However, in this research, we only installed and characterized commercial back-sheet-type silicon solar modules. The modules were installed together with IP68 class junction boxes and cables with waterproof capability. For the reference modules installed on land (1607 W), the installation angles were set to 0° and 30°, the salt-farm parallel solar power plant module (1628 W) was installed at 0°, and the comparative evaluation was made. The power generation of the tilted module was multiplied by a normalized factor of 0.987 to compare the power generation. According to our design and experiments, we successfully installed the pilot system at our test bed site. More feasibility and reliability tests will be carried out, and we will present the results in our next publication.

Fig. 8 shows a comparison of power generation of conventional and salt farm modules in one day (August 18, 2018), as well as the temperature of the outdoors, water, land module, and salt-farm module on the same day. As can be seen in Fig. 8 (a), the typical data show improvement of the generation amount as compared with the land because of the cooling effect of the seawater. In the morning, the modules installed on land showed better electricity generation; but after 11:40 a.m., the salt farm PV modules indicated higher electricity generation. The electricity generation of the land-installed modules and the salt-farm modules were, respectively, 8.18 and 8.60 kWh (normalized 8.49 kWh) on average. Therefore, it can be said that the salt farm modules showed higher electricity generation than that of the land-installed modules mainly because of the cooling effect of the seawater. The highest temperature on that day was 32.9 °C, and the highest temperature of the salt water was 43.7 °C. The seawater temperature began to rise more rapidly than the ambient temperature from 9:00 a.m., and it rose by more than 12 °C from the maximum outside air temperature. This means that the heat absorbed by the module was effectively dissipated through the water. The temperature of the module increased to 51.1 °C at sea level and to 39.1 °C for the torsion as the outside temperature increased. The maximum difference between modules was 15 °C. The cooling effect of the salt-farm modules was observed continuously in the morning, but the lower power generation was caused by the incidence angle loss relative to that on land. The cooling effect could be maximized by circulating the water or by re-introducing low temperature salt water by suppressing the rising water temperature.

Fig. 9 shows a comparison of daily power generation of the PV modules at the salt farm with the land module (reference) for the days when the depth of the salt-dedicated module was maintained at 2–3 cm from May to August 2018 (minimum water depth was maintained for 7 days or more). The figure shows the ratio of the salt farm to the land-installed module electricity generation rate with the applied normalized factor. The salt farm modules showed rates of 108% in May to June, ~118% in July, ~100% in August, and 91.7% in September relative to that of the land-installed salt farm module. As discussed above, the cooling effect of the seawater provides better electricity generation in the salt farm modules. The electricity generation by the salt farm modules was similar to that in August and lower than that in September for the land-installed modules. We assume that this is mainly due to the deposition of biofloc or foreign matter on the surface of the module. Therefore, it is highly important for achieving maximum power generation to keep the surface of the salt farm modules clean. Regarding to electrochemically driven degradation effects, we keep monitoring the power output of the system.

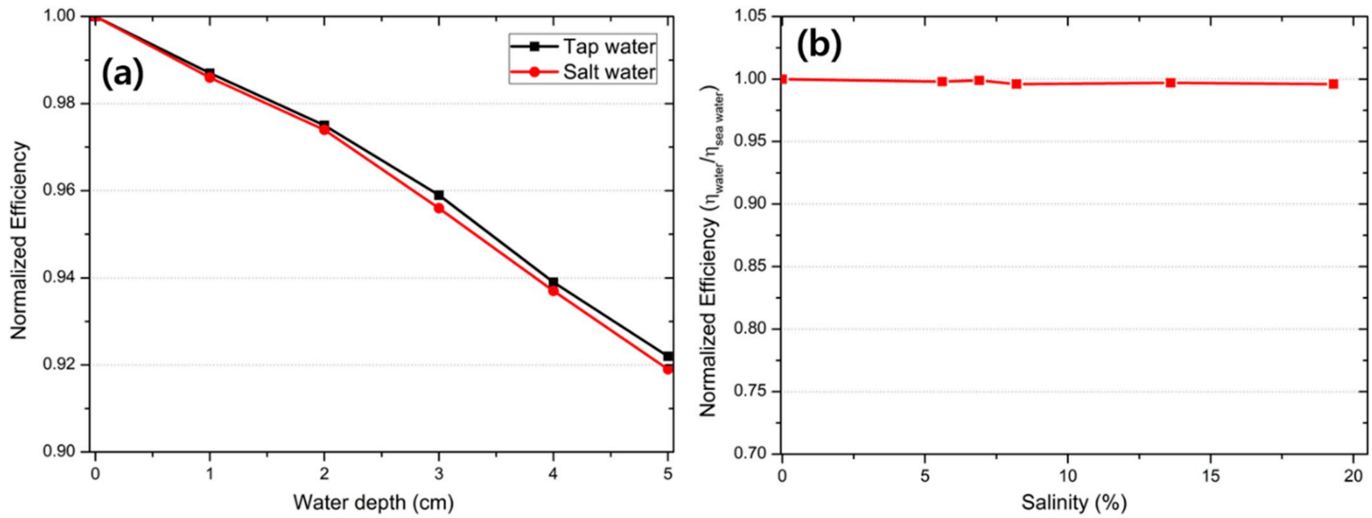

Fig. 6. (a) Normalized efficiency of solar modules sunk in tap water and salt water at different depth, and (b) normalized efficiency of solar module at different salinity.

Fig. 7. Image of the salt farm parallel solar power system test bed.

In order to predict the annual electricity generation of the modules installed on land and in the solar farm, we conducted simulations using SolarPro PV simulation software (Laplace System, USA). The meteorological conditions were based on the Meteorological Agency data of Mokpo, Jeollanam-do. We also used the meteorological data collected at the salt farm test site, and the temperature of the salt farm module collected from the test site in order to accurately predict the temperature of the salt module used. Fig. 9 (b) shows the simulation results. The module error rate of the predicted module temperature was 5.6%, which was able to reliably predict the module temperature. The decrease in solar radiation due to the depth of 2 cm was estimated by applying 4.46% predicted from Table 1. Similar to the actual measurement data shown in Fig. 9 (a), the electricity generation rate of the salt farm modules was higher than that of the land-installed modules (0°, reference) in all months. It can be seen that the seawater contributed more to the increase in the module performance than did the absorption loss due to water by maintaining a height of 2 cm above the module. The land-installed modules (30°) showed better power generation than the salt farm from September to March because the incident angle of the sun was lower during that season. However, in the other months, the salt farm modules showed higher power generation rate, and the total annual power generation rates were similar in the salt farm modules (1910 kWh) and the land-installed modules (30°) (1962 kWh). Therefore, it can be said that the power generation of the salt-farm parallel system is comparable to that of conventional solar power plants.

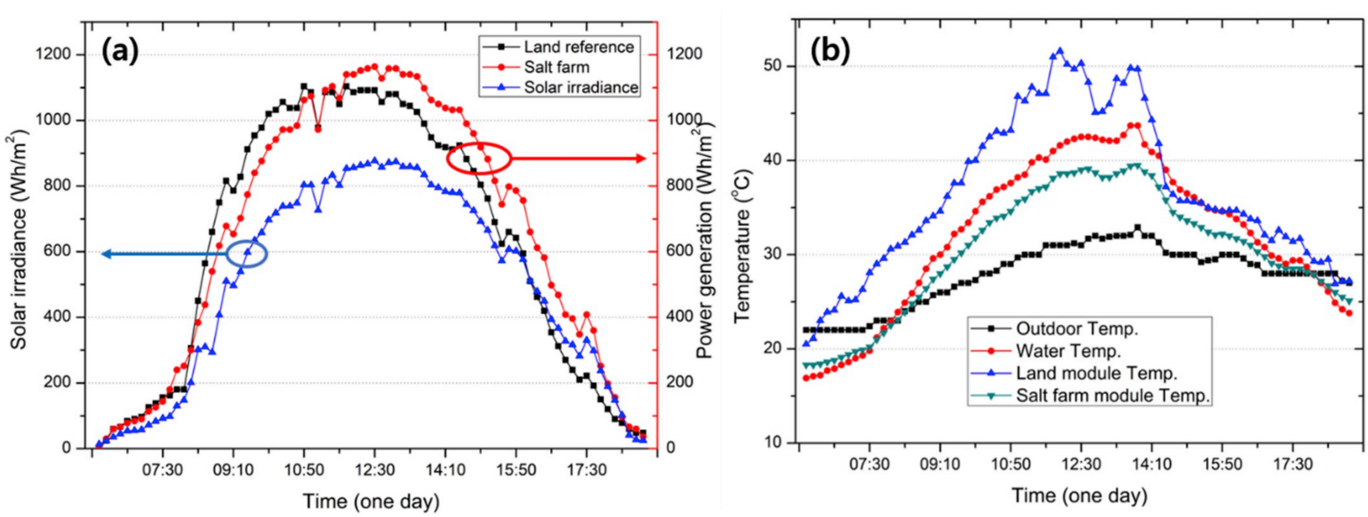

Fig. 8. (a) Comparison power generation of conventional and salt farm module at a day (18 Aug 2018), and (b) the temperature of outdoor, water, land module and salt farm module (2 cm above the module front) on 18 Aug 2018.

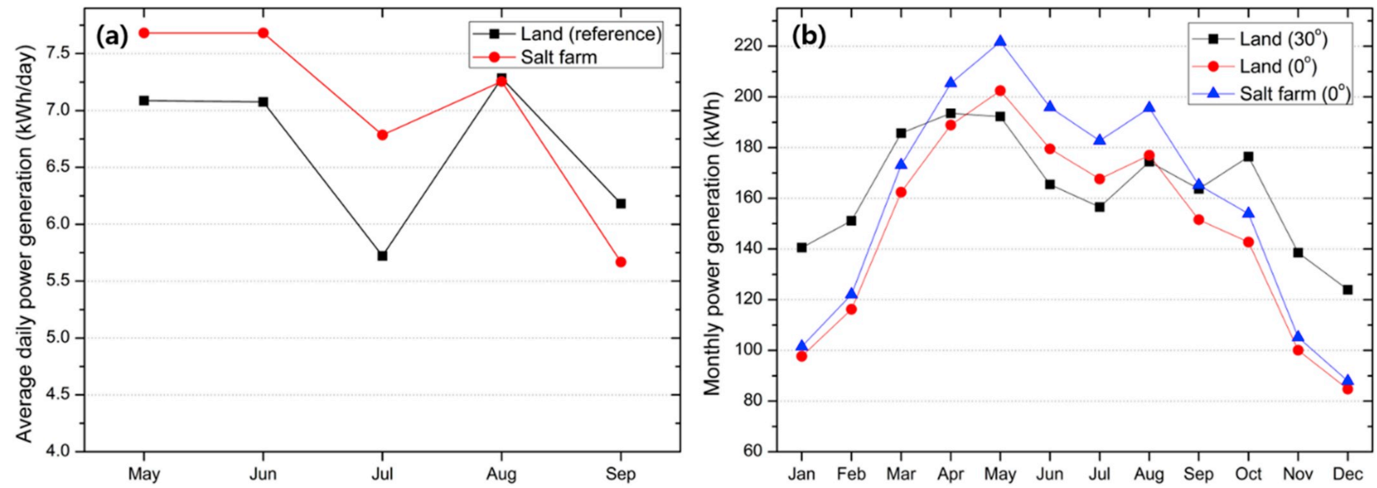

Fig. 9. (a) System yield and performance ratio (May ~ Sep 2018, sea water level 2 cm) and (b) the results of power generation simulations.

3.3. Issues encountered during operation of the parallel system

A variety of issues arose during the running of the salt farm-parallel solar power system. The solar farm located on the coast poses the following difficulties with operating the PV system: The potential-induced degradation (PID) caused by the diffusion of Na ions in the general module degrades the performance PV modules. Therefore, the probability of PID occurrence in the parallel system is high because the seawater contains a large amount of Na ions. It is also questionable whether electrostatic induction on the module front may affect the crystallization of salt and the output. The quality and safety of salt is also something we needed to secure. In order to keep salt water in the upper part of the module for the long term, the entire system should have resistance to salt, be stable to ultraviolet, have a low thermal expansion coefficient, and be harmless to the human body. As shown in Fig. 9, it is considered that the decrease in the actual operation power generation compared with the computer simulation result may be due to the deposition of biofloc or foreign matter on the surface of the module. Therefore, maintaining the surface cleanliness is a major issue. As the water depth increases, it becomes clear that the power generation rate decreases to ~1%/cm, and it is necessary to set the cooling effect to larger than the power generation rate decrease at a low water depth (about 2–3 cm). In other words, it is essential to improve the power generation by managing the pollution of the surface of the photovoltaic module and by maintaining a low water depth of about 2–3 cm.

4. Conclusion

In this research, we proposed a salt farm parallel solar power plant, which can produce both salt and electricity at the same site. The FRP seawater vessel for the pilot system was prepared for efficient maintenance, and PV modules were installed on the water tank. We found that measured spectral solar irradiance at different depths from sea level decreased within the 600 nm wavelength range, but solar irradiation at 300–600 nm did not change along with the depth. The overall efficiency reduction is mainly due to current reduction by loss of solar irradiance. We also found that water depth and temperature have no strong correlation, and that they independently affect the module performance. Moreover, the salinity of the seawater has no influence on the performance of the PV modules in the short term. According to our design and experiments, we successfully installed the pilot system at our test bed site. From the field tests, we found that salt-farm modules showed electricity generation higher than that of the land-installed modules mainly because of the cooling effect of the seawater. However, in long-term operation, the salt farm modules showed lower power generation because of the deposition of bioplag or foreign matter on the surface of the module. Therefore, it is important to keep the surface of the salt-farm modules clean. From the power prediction simulations, we found that the electricity generation rate of the salt-farm modules was higher than that of the land-installed modules (0°, reference) in all months. It can be seen that the seawater contributes more to the increase in the module performance than does the absorption loss due to water by maintaining a height of 2 cm above the module. The land-installed modules (30°) showed power generation better than that of the salt farm from September to March because the incident angle of the sun was lower during that season, but the salt-farm modules showed higher power generation in the other months. Finally, the total annual power generation rates were similar to each other. Therefore, it can be said that the power generation of the salt farm module is comparable to that of conventional solar power plants. More feasibility and reliability tests will be carried out, and we will present the results soon.

Acknowledgement

This work was supported by the Korea Electric Power Research Institute (KEPRI) grant funded by Korea Electric Power Corporation (KEPCO) (R16EA09).

Appendix A. Supplementary data

Supplementary data to this article can be found online at https://doi.org/10.1016/j.solmat.2019.110234.

References

[1] R.H. Moss, et al., The next generation of scenarios for climate change research and assessment, Nature 463 (7282) (2010) 747–756.
[2] P. Droege, Renewable Energy and the City : Urban Life in an Age of Fossil, vol. 22, 2002, pp. 87–99, no. 2.
[3] O.H. Hohmeyer, S. Bohm, Trends toward 100 % Renewable Electricity Supply in Germany and Europe : a Paradigm Shift, 2014.
[4] K.J. Chalvatzis, A. Ioannidis, Energy supply security in southern Europe and Ireland, Energy Procedia 105 (2006) (2017) 2916–2922.
[5] V. Duscha, et al., Renewable energy deployment in Europe up to 2030 and the aim of a triple dividend, Energy Policy 95 (2016) 314–323.
[6] 2016 Energy Info Korea, 2016.
[7] J. Khan, M.H. Arsalan, "Solar power technologies for sustainable electricity generation – a review, Renew. Sustain. Energy Rev. 55 (2016) 414–425.
[8] H. Yang, S. Lim, S. Yoo, The Environmental Costs of Photovoltaic Power Plants in South Korea : A Choice Experiment Study, 2017, pp. 1–13.
[9] I. Capellán-pérez, C. De Castro, I. Arto, Assessing vulnerabilities and limits in the transition to renewable energies : land requirements under 100 % solar energy scenarios, Renew. Sustain. Energy Rev. 77 (2017) 760–782, no. December 2016.
[10] C. Angeli, E. Leonardi, A One-Dimensional Numerical Study of the Salt Diffusion in a Salinity-Gradient Solar Pond, vol. 47, 2004, pp. 1–10.

[11] E. Skoplaki, J.A. Palyvos, On the temperature dependence of photovoltaic module electrical performance : a review of efficiency/power correlations, Sol. Energy 83 (5) (2009) 614–624.

[12] S. Dubey, J.N. Sarvaiya, B. Seshadri, Temperature dependent photovoltaic (PV) efficiency and its effect on PV production in the world a review, Energy Procedia 33 (2013) 311–321.

[13] S. Odeh, M. Behnia, Improving Photovoltaic Module Efficiency Using Water Cooling, 2009 no. May 2017.

[14] Y. Kageshima, T. Shinagawa, T. Kuwata, J. Nakata, A Miniature Solar Device for Overall Water Splitting Consisting of Series- Connected Spherical Silicon Solar Cells, *Nat. Publ. Gr.*, 2016, pp. 1–12, no. April.

[15] W.S. Pegau, D. Gray, J.R. V Zaneveld, Absorption and Attenuation of Visible and Near-Infrared Light in Water : Dependence on Temperature and Salinity, vol. 36, 1997, pp. 6035–6046, no. 24.